Flatness-based longitudinal vehicle control with embedded torque constraint

Hugues Mounier, Silviu-Iulian Niculescu, Arben Cela, Marcel Stefan Geamanu

▶ To cite this version:

HAL Id: hal-01705876

https://hal.science/hal-01705876

Submitted on 9 Feb 2018

Flatness based longitudinal vehicle control with embedded torque constraint

HUGUES MOUNIER[†]*, SILVIU-IULIAN NICULESCU[†], ARBEN CELA[‡] AND MARCEL STEFAN GEAMANU[††]

[†] *Laboratoire des Signaux et Systèmes, CentraleSupélec, 3, rue Joliot Curie, 91192 Gif sur Yvette, FRANCE. (e-mails: {hugues.mounier,silviu.niculescu}@l2s.centralesupelec.fr)* [‡] *UPE ESIEE Paris, 2 boulevard Blaise Pascal, 93162 Noisy le Grand, FRANCE. (e-mail: a.cela@esiee.fr)* [††] *Renexter, B-dul Iuliu Maniu, nr. 7, corp B, et. 2, sector 6, Bucuresti, ROMANIA. (e-mail: marcel.geamanu-renexter@renault.com)*

This paper aims at establishing a simple yet efficient solution to the problem of trajectory tracking with input constraint of a nonlinear longitudinal vehicle model. We make use of differential flatness, by embedding the constraint into the reference trajectory design.

Keywords: flatness based control, automotive control, input constraints

1. Introduction

The aim of this paper is to come up with simple yet efficient control techniques for vehicle longitudinal speed control with constraint on its torque. More precisely, we consider a longitudinal nonlinear model including a simple adherence/friction law (see, e.g. (Ellis, 1969; Gillespie, 1992; Kiencke and Nielsen, 2000; Mitschke, Manfred ; Wallentowitz, 2004; Rajamani, 2011)). For this model, we consider the problem of tracking a reference speed trajectory with constraint on the input torque. Traditional treatment of such a problem include model predictive control (Li et al., 2011) and use of optimisation techniques (Hsu and Chen, 2013; Hsu et al., 2010) Some other works use adaptive anti-windup techniques (Kahveci and Ioannou, 2010; Tarbouriech and Turner, 2009), saturated inputs (Valmorbida et al., 2013) to name a few.

The constraint is embedded in the flat output trajectory design. Thus, the closed loop tracking controller naturally satisfies the required constraint, without the recourse to costly optimisation procedure. A key advantage of the advocated technique is that the physical meaning is kept throughout the whole process, a feature often lost in MPC or other optimisation based techniques.

More precisely, a dynamical system with m inputs is differentially flat (Fliess et al., 1995) if there exists a so-called flat output $\boldsymbol{\omega}$ with m components $\boldsymbol{\omega} = (\omega_1, \ldots, \omega_m)$ such that: first, these components are functions of the system's variables (endogenous character); second, the ω_is are differentially independent, i.e. they don't satisfy a differential equation involving themselves only (independent character); third, all the system's variables can be expressed as nonlinear functions of the ω_is and of a finite number of their derivatives (parametrisation property).

Thus, when a system variable is subject to a constraint, the latter is directly translated into a flat output constraint, thanks to the parametrisation property. The tracking problem with constraints is thus elaborated in two steps: first design a flat output reference trajectory $\boldsymbol{\omega}_r$ satisfying all the required constraints; second, design a closed loop feedback control law ensuring the tracking of $\boldsymbol{\omega}_r$ with stability. The constraints satisfaction is ensured by design, since it is embedded in the reference trajectory

---

*Corresponding author.

elaboration process.

The involved constraints can be given on any system variable, since all the system is parametrised by the flat output. The constraint is enforced on the reference variables, and is ensured practically on the actual variables since the tracking error is meant to tend to zero, in general exponentially.

Ensuring the constraints on the flat output is simplified by specialising the flat output reference trajectory to specific classes of functions with convenient properties, such as closedness wrt differentiation or being solution of a differential equation.

To the best of the author's knowledge, almost all the current work on differentially flat systems with constraints is managed through optimisation procedures (Chamseddine et al., 2013; Faiz et al., 2001; Flores and Milam, 2006; Keck et al., 2015; Petit and Sciarretta, 2011; Ross and Fahroo, 2004; Tsuei and Milam, 2016; Walambe et al., 2016). In (Löwis and Rudolph, 2003), no optimisation technique is used, but the flat output trajectory is not known on advance; thus, the trajectory is built step by step, by concatenating pieces The only work partially related to our approach is (Ruppel et al., 2011), where the constraints appear solely on derivatives of the flat output, which is specialised to piecewise polynomial functions. Preliminary results related to the present one have been presented for linear systems with delays in (Bekcheva et al., 2017), and for an Euler Bernoulli beam in (Bekcheva et al., 2015). Other works related to the present theme include differential flatness based techniques for longitudinal and lateral vehicle dynamics (Menhour et al., 2014).

The paper is organised as follows. In the next Section, the model is recalled. In Section 3, the flatness of the model is established, and a closed loop feedback tracking controller is given in Section 4. The torque constraint management is dealt with in Section 5.

2. Longitudinal model

The equations of the vehicle dynamics can be written as follows (see, e.g. (Ellis, 1969; Gillespie, 1992; Kiencke and Nielsen, 2000; Mitschke, Manfred ; Wallentowitz, 2004; Rajamani, 2011)) :

$$m\dot{V}_x = F_x \tag{2.1a}$$

$$I_w\dot{\omega} = RT - rF_x - F_o \tag{2.1b}$$

with the following slip ratio and forces :

$$F_x = \mu_x(\lambda)F_z, \qquad \lambda = \frac{V_x - r\omega}{\max(V_x, r\omega)} \tag{2.2a}$$

$$F_z = mg \tag{2.2b}$$

$$F_o = -F_a - F_s \tag{2.2c}$$

$$R_x = mgC_r, \qquad F_a = \frac{\rho\, C_a A V_x^2}{2}, \quad F_s = mg\sin\alpha \tag{2.2d}$$

The notations for the model (2.1a)–(2.1b) are: V_x is the longitudinal speed of the vehicle, m its mass, F_x the longitudinal tire force, I_w inertia moment of the wheel, ω angular wheel speed, R the damping coefficient of the drive-line, T the engine torque, r the effective tire radius, F_o the other forces exterted on the car body.

The expressions of the forces are given in Equations (2.2a)–(2.2d), with the following notations: μ_x is the adherence function, F_z the normal force on the tire, λ the slip ratio, g the gravity constant, R_x the rolling resistance force, F_a the longitudinal aerodynamic drag force, ρ is the air volumic mass, A is
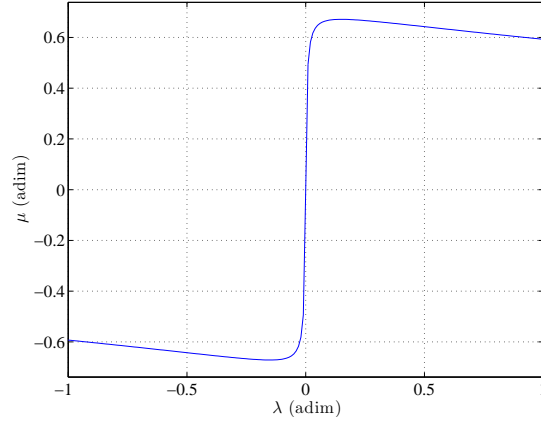
FIG. 1: Adherence function $\mu(\lambda)$.

frontal area of the vehicle, C_a is the drag coefficient, F_s the force due to the road slope, and α the road slope angle.

A possible model for $\mu_x(\lambda)$ introduced by Kiencke and Daiß and depicted in Figure 1, is given by the function:

$$\mu_x(\lambda) = \frac{a\lambda}{b + c|\lambda| + \lambda^2} \tag{2.3}$$

One easily obtains that the maximum μ^* of such a curve occurs at λ^* with:

$$\lambda^* = \sqrt{b}, \quad \mu^* = \frac{a}{c + 2\sqrt{b}}$$

Conversely, the constants a, b, c can be expressed as functions of $\mu^* \lambda^*$ and μ_1:

$$a = \frac{\mu^* \mu_1 (1 - \lambda^*)^2}{\mu^* - \mu_1}, \quad b = \lambda^{*2}, \quad c = \frac{\mu_1 (1 + \lambda^{*2}) - 2\mu^* \lambda^*}{\mu^* - \mu_1}$$

where $\mu_1 = \mu(1)$ is the value of the function μ at $\lambda = 1$ (i.e. at wheel lock). Note that a and b are strictly positive constants.

REMARK 2.1 Another, quite popular, model is the Pacejka one (Bakker et al., 1987; Pacejka, 2006). We have not used the latter, for simplicity reasons, but a similar, although more complex, analysis could be made with Pacejka's model.

The measured outputs are traditionally the wheel speed (e.g. through ABS encoders). We shall here suppose that the speed V_x of the vehicle's center of gravity is either measured or reconstructed via an observer or an estimator (see, e.g. a previous work of some author of the present paper (Villagra et al., 2008)).

3. Differential flatness of the model

The model (2.1) is trivially flat, with flat output V_x. Indeed,

$$\dot{V}_x = g\mu_x(\lambda) \tag{3.1}$$

Then,

$$\lambda = \mu^{-1}\left(\frac{\dot{V}_x}{g}\right) \tag{3.2}$$

Now one has to distinguish two acceleration and deceleration cases (implied by the form of λ in (2.2a)):

- Acceleration case, where $r\omega \geqslant V_x$

$$\lambda = \frac{V_x}{r\omega} - 1 = \mu^{-1}\left(\frac{\dot{V}_x}{g}\right)$$

  Hence

$$\omega = \frac{V_x}{r\left[1 + \mu^{-1}\left(\frac{\dot{V}_x}{g}\right)\right]} \tag{3.3}$$

  And thus

$$\ddot{V}_x = g\mu'_x(\lambda)\dot{\lambda} = g\mu'_x(\lambda)\frac{1}{r\omega^2}\left(\omega\dot{V}_x - \dot{\omega}V_x\right)$$

- Deceleration case, where $r\omega \leqslant V_x$

$$\lambda = 1 - \frac{r\omega}{V_x} = \mu^{-1}\left(\frac{\dot{V}_x}{g}\right)$$

  Hence

$$\omega = \frac{V_x}{r}\left[1 - \mu^{-1}\left(\frac{\dot{V}_x}{g}\right)\right] \tag{3.4}$$

  And thus

$$\ddot{V}_x = g\mu'_x(\lambda)\dot{\lambda} = g\mu'_x(\lambda)\frac{r}{V_x^2}\left(\omega\dot{V}_x - \dot{\omega}V_x\right)$$

Thus, one has the following dynamics in V_x:

$$\ddot{V}_x = \frac{g\mu'_x}{\max\left(r\omega^2, \frac{V_x^2}{r}\right)}\left[\omega\dot{V}_x + \frac{V_x}{I_w}\left(mr\dot{V}_x + F_o + RT\right)\right] \tag{3.5}$$

and the control input T is then obtained as

$$T = \frac{1}{R}\left[\left(mr + \frac{I_w\omega}{V_x}\right)\dot{V}_x + F_o - \frac{I_w\max\left(r^2\omega^2, V_x^2\right)}{grV_x\mu'_x}\ddot{V}_x\right] \tag{3.6}$$

REMARK 3.1 The reader could have the (quite normal) feeling that the laws (3.3) and (3.4) yield a discontinuity when the vehicle switches from acceleration to deceleration (leading to a chattering like phenomenon). First note that this can only occur at extremely low slip, i.e. when $r\omega - V_x \ll 1$, where the $\mu()$ curve is in the linear zone (and thus the μ^{-1} also); thus

$$\mu^{-1}\left(\frac{\dot{V}_x}{g}\right) \approx \beta\frac{\dot{V}_x}{g}$$

Moreover, when the vehicle switches from acceleration to deceleration (or vice-versa), one has $|\dot{V}_x| \ll 1$. Thus, in (3.3), one has

$$\frac{1}{1+\mu^{-1}\left(\frac{\dot{V}_x}{g}\right)} = 1 - \mu^{-1}\left(\frac{\dot{V}_x}{g}\right) + o\left(\left(\frac{\dot{V}_x}{g}\right)^2\right)$$

Thus, the expression of ω is

$$\omega = \frac{V_x}{r\left[1+\mu^{-1}\left(\frac{\dot{V}_x}{g}\right)\right]} = \frac{V_x}{r}\left[1 - \mu^{-1}\left(\frac{\dot{V}_x}{g}\right) + o\left(\left(\frac{\dot{V}_x}{g}\right)^2\right)\right]$$

whose term in $o((V_x/g)^2)$ is exactly the one of (3.4). Thus, in case of acceleration-deceleration switching, the expression of ω is continuous and differentiable.

4. Trajectory tracking

4.1 *Trajectory tracking control law*

Recalling the flat output dynamics (3.5), and setting the right member equal to a new input v, one obtains the linearizing feedback

$$\omega\dot{V}_x + \frac{V_x}{I_w}\left(mr\dot{V}_x + F_o + RT\right) = \frac{\max\left(r^2\omega^2, V_x^2\right)}{gr\mu_x'}v$$

tranforming the flat output dynamics (3.5) to

$$\ddot{V}_x = v$$

Setting the new input v to

$$v = \ddot{V}_{xr} - K_p e_{V_x} - K_d \dot{e}_{V_x}, \quad e_{V_x} = V_x - V_{xr}$$

with $K_p, K_d > 0$ yield an exponentially stable error dynamics. The original input is then obtained as

$$T = \frac{1}{R}\left[\left(mr + \frac{I_w\omega}{V_x}\right)\dot{V}_x + F_o - \frac{I_w\max\left(r^2\omega^2, V_x^2\right)}{grV_x\mu_x'}v\right] \tag{4.1}$$

$$v = \ddot{V}_{xr} - K_p e_{V_x} - K_d \dot{e}_{V_x} \tag{4.2}$$

REMARK 4.1 Note that, in (4.2), one could have used equally a second order sliding mode or a model free control law, for instance, in order to gain in robustness.

4.1.1   *Open and closed loop tracking.*   Let V_{xr} a reference trajectory for the flat output V_x. Denoting by T_r the following open loop control law, one has by direct substitution from (3.6):

$$T_r = \frac{1}{R} \left[\left(mr + \frac{I_w \omega_r}{V_{xr}} \right) \dot{V}_{xr} + F_o - \frac{I_w \max \left(r^2 \omega_r^2, V_{xr}^2 \right)}{g r V_x \mu'_{xr}} \ddot{V}_{xr} \right] \tag{4.3}$$

Thus, the Equations (4.1)–(4.2) can be rewritten as

$$T = T_r - \frac{1}{R} \left(K_p e_{V_x} + K_d \dot{e}_{V_x} \right) \tag{4.4}$$

We thus see that, if the error e_{V_x} and its derivative $\dot{e}_{V_x}$ remain small (which is the case when the tacking performance is good), the closed loop torque T remains close to the open loop one T_r.

4.2   *Trajectory tracking scenario*

4.2.1   *Trajectory form.*   We shall choose a trajectory $V_{xr}(t)$ of the following form

$$V_{xr}(t) = \Omega_{\boldsymbol{p}_u, \boldsymbol{p}_d}(t) = \Theta_{\boldsymbol{p}_u}(t) - \Theta_{\boldsymbol{p}_d}(t) \tag{4.5}$$

$$\Theta_{\boldsymbol{p}*}(t) = \frac{V_{h*} - V_{l*}}{2(t_{e*} - t_{b*})} \left(\text{logCh}_{\sigma_*}(t - t_{b*}) + \text{logCh}_{-\sigma_*}(t - t_{e*}) \right) + \frac{V_{h*} - V_{l*}}{2} \tag{4.6}$$

$$\text{logCh}_\sigma(t) = \frac{1}{\sigma} \log \left(\cosh(\sigma t) \right)$$

$$\boldsymbol{p}_* \in \{ \boldsymbol{p}_u, \boldsymbol{p}_d \}, \quad \boldsymbol{p}_u = (t_{bu}, t_{eu}, V_{lu}, V_{hu}, \sigma_u), \quad \boldsymbol{p}_d = (t_{bd}, t_{ed}, V_{ld}, V_{hd}, \sigma_d)$$

The forms of $\Omega_{\boldsymbol{p}_u, \boldsymbol{p}_d}$ and $\Theta_{\boldsymbol{p}}$ are depicted in Figures 2 and 3. The speeds V_{l*} and V_{h*} are the beginning and reached speeds, respectively; t_{b*} and t_{e*} are the beginning and ending times of speed change. The real σ_* is a stiffness parameter: the higher σ_*, the closer $\text{logCh}_{\sigma_*}(t)$ is from $|t|$.

REMARK 4.2 One could have chosen a tanh-like trajectory for V_{xr}. The chosen form (which amounts to a combination of primitives of tanh) is a smooth (in fact entire) approximation of a trajectory yielding a piecewise constant acceleration. The difference $t_{e*} - t_{b*}$ is related to the acceleration, while the stiffness σ is related to the jerk. A tanh-like trajectory would furnish only a single design parameter (the stiffness).
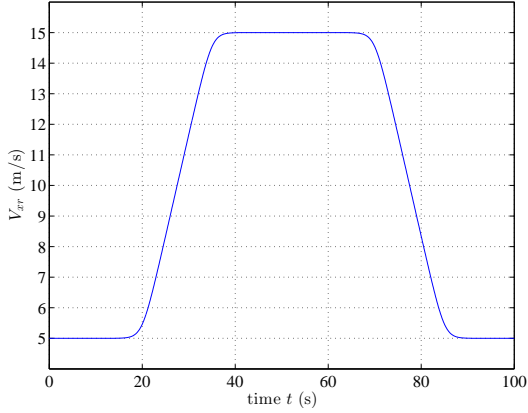
The associated trajectory parameters are: $\sigma = 0.5$, $t_{bu} = 20s$, $t_{eu} = 35s$, $t_{bd} = 70s$, $t_{ed} = 85s$.

4.2.2   *A physical constraint.*   Using Eq. (2.1a), p. 2, we have

$$\dot{V}_x = g \mu_x(\lambda)$$

Since the μ_x curve is imposed by the tyre/ground physics, we should ensure that $\dot{V}_x$ does not exceed the maximum (resp. minimum) of $g\mu_x$. In other words, the chosen trajectory will be such that the physical constraint

$$\left| \dot{V}_{xr} \right| \leqslant g \max_{\lambda \in [-1,1]} \left(\mu_x(\lambda) \right) \tag{4.7}$$

FIG. 2: An example of $V_{xr}(t) = \Omega_{\boldsymbol{p}_u, \boldsymbol{p}_d}(t)$ trajectory.
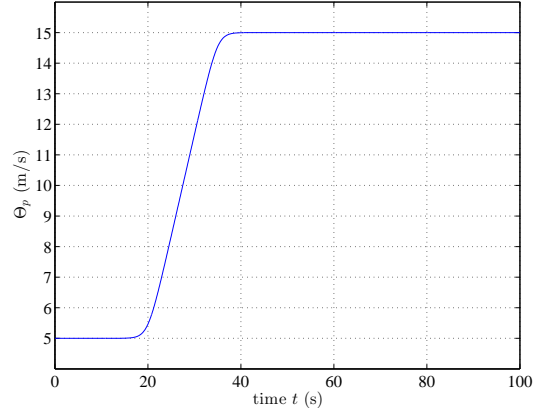
FIG. 3: An example of $\Theta_{\boldsymbol{p}}(t)$ function.

is met, where

$$\max_{\lambda \in [-1,1]} (\mu_x(\lambda)) = \mu_x(\lambda^*) = \mu^*$$

is given by (see Eq. (2.3) and below)

$$\mu^* = \frac{a}{c + 2\sqrt{b}}, \quad \text{with} \quad \lambda^* = \sqrt{b}$$

We shall consider the following

$$\max_{t \in \mathbb{R}} \left| \dot{V}_{xr}(t) \right| = g(\mu^* - \varepsilon_{\mu_x}) \triangleq g\mu_M \tag{4.8}$$

where ε_{μ_x} is such that $\varepsilon_{\mu_x}/\mu^* \ll 1$. This corresponds to

$$\lambda_M = \mu^{-1}(\mu_M) = \lambda^* - \varepsilon_\lambda \tag{4.9}$$

where ε_λ is such that $\varepsilon_\lambda/\lambda^* \ll 1$.

4.2.3 *Trajectory tracking.* The trajectory tracking of $V_{xr} = \Omega_{\boldsymbol{p}_u, \boldsymbol{p}_d}$ is depicted in Figures 4 and 5. The chosen parameters are the following: initial conditions $V_{x0} = 5$m/s, $\omega_0 = 16.67$rad/s, starting speed $V_{lu} = V_{ld} = 5$m/s, reached speed $V_{hu} = V_{hd} = 15$m/s. We see on Fig. 4 and 5 that the trajectory tracking is achieved with a very good precision, since the maximum error $V_x - V_{xr}$ in Fig. 5 is $2.055.10^{-5}$. The slip ratio λ and the adherence function $\mu(\lambda)$ are plotted in Figures 6 and 7. Remark that this slip ratio λ remains very small (the maximum of λ is $4.613.10^{-4}$). The parameters of the function $\mu(\lambda)$ are: $a = 3.661$, $b = 0.022$, $c = 5.153$.
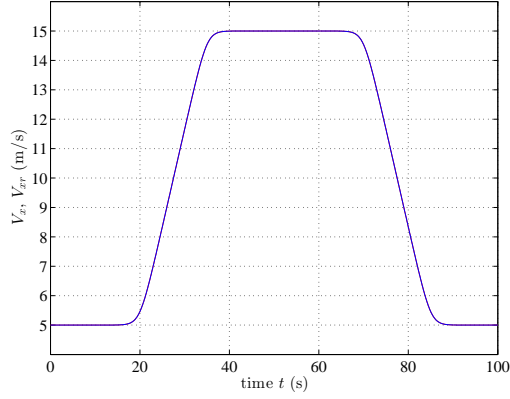
H. MOUNIER et al.

FIG. 4: Speed trajectory tracking; in blue V_x and in red V_{xr}, standard trajectory.
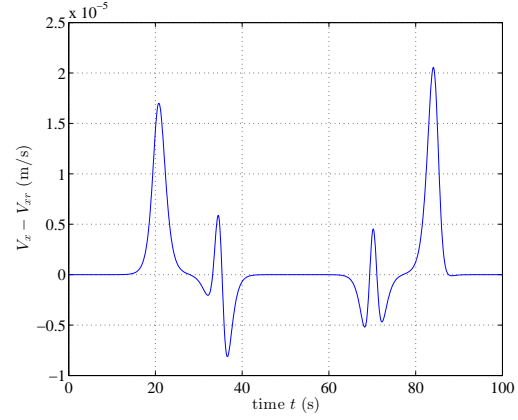

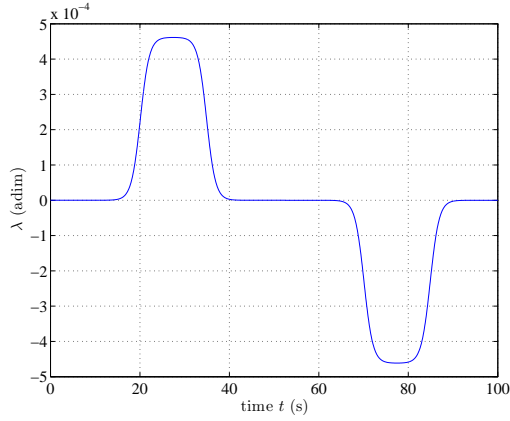FIG. 5: Speed trajectory tracking error $V_x - V_{xr}$, standard trajectory.

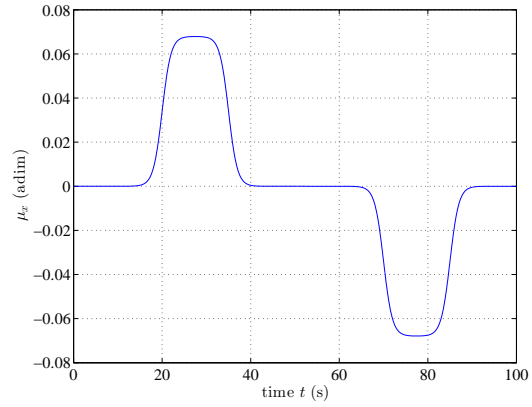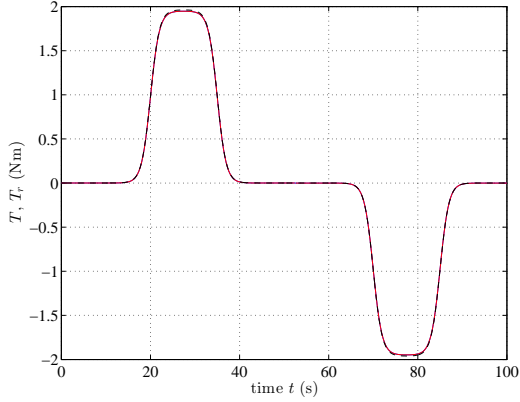FIG. 6: Slip ratio λ, standard trajectory.

FIG. 7: Adherence μ_x, standard trajectory.

The control law T and the error $T - T_r$ are depicted in Figures 8 and 9. The chosen feedback gains are: $K_p = 200$, $K_d = 10$. Finally, the closed loop torque T is very close to the open loop torque T_r, as can be seen on Fig. 9: the maximum error (in absolute value) $T - T_r$ is $-1.4.10^{-6}$.

FIG. 8: Closed loop control T, standard trajectory.
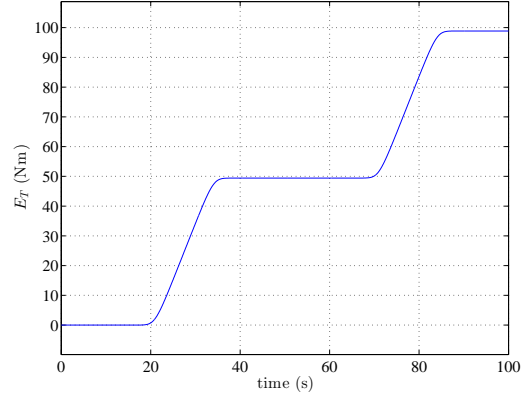
FIG. 9: Control error $T - T_r$, standard trajectory.

5. Torque constraint management

Since the constraints will be expressed in terms of the flat output V_x and its derivatives, we have to compute analytically the first derivatives of V_x.

5.1 *Trajectory first derivatives*

The derivatives of Ω are the following:

$$\dot{V}_{xr} = \dot{\Omega}_{\boldsymbol{p}_u,\boldsymbol{p}_d}(t) = \frac{V_{hu} - V_{lu}}{2(t_{eu} - t_{bu})} \left(\tanh\left(\sigma_u(t - t_{bu}) \right) + \tanh\left(-\sigma_u(t - t_{eu}) \right) \right) -$$
$$\frac{V_{hd} - V_{ld}}{2(t_{ed} - t_{bd})} \left(\tanh\left(\sigma_d(t - t_{bd}) \right) + \tanh\left(-\sigma_d(t - t_{ed}) \right) \right) \tag{5.1}$$

$$\ddot{V}_{xr} = \ddot{\Omega}_{\boldsymbol{p}_u,\boldsymbol{p}_d}(t) = \frac{\sigma_u(V_{hu} - V_{lu})}{2(t_{eu} - t_{bu})} \left(\tanh^2\left(-\sigma_u(t - t_{eu}) \right) - \tanh^2\left(\sigma_u(t - t_{bu}) \right) \right) -$$
$$\frac{\sigma_d(V_{hd} - V_{ld})}{2(t_{ed} - t_{bd})} \left(\tanh^2\left(\sigma_d(t - t_{ed}) \right) - \tanh^2\left(-\sigma_d(t - t_{bd}) \right) \right) \tag{5.2}$$

For the example depicted in Figure 2, we get the derivatives in Figures 10 and 11. The maximum and minimum of $\dot{\Omega}_{\boldsymbol{p}_u,\boldsymbol{p}_d}$ and $\ddot{\Omega}_{\boldsymbol{p}_u,\boldsymbol{p}_d}$ are

$$\max(\dot{\Omega}_{\boldsymbol{p}_u,\boldsymbol{p}_d}(t)) = \frac{V_{hu} - V_{lu}}{2(t_{eu} - t_{bu})}, \qquad \min(\dot{\Omega}_{\boldsymbol{p}_u,\boldsymbol{p}_d}(t)) = -\frac{V_{hd} - V_{ld}}{2(t_{ed} - t_{bd})} \tag{5.3}$$

$$\max(\ddot{\Omega}_{\boldsymbol{p}_u,\boldsymbol{p}_d}(t)) = \max\left(\frac{\sigma_u(V_{hu} - V_{lu})}{2(t_{eu} - t_{bu})}, \frac{\sigma_d(V_{hd} - V_{ld})}{2(t_{ed} - t_{bd})} \right) \tag{5.4}$$

$$\min(\ddot{\Omega}_{\boldsymbol{p}_u,\boldsymbol{p}_d}(t)) = -\max\left(\frac{\sigma_u(V_{hu} - V_{lu})}{2(t_{eu} - t_{bu})}, \frac{\sigma_d(V_{hd} - V_{ld})}{2(t_{ed} - t_{bd})} \right) \tag{5.5}$$
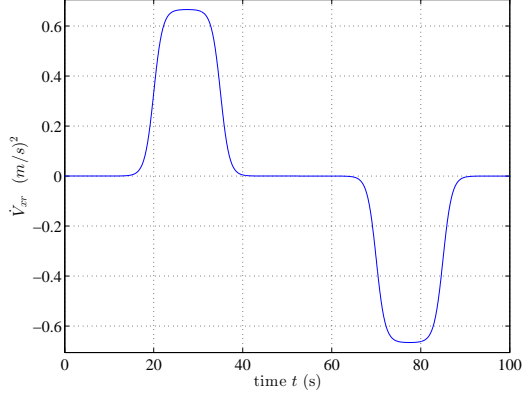
FIG. 10: The first derivative $\dot{V}_{xr} = \dot{\Omega}_{\boldsymbol{p}_u, \boldsymbol{p}_d}$ (acceleration).
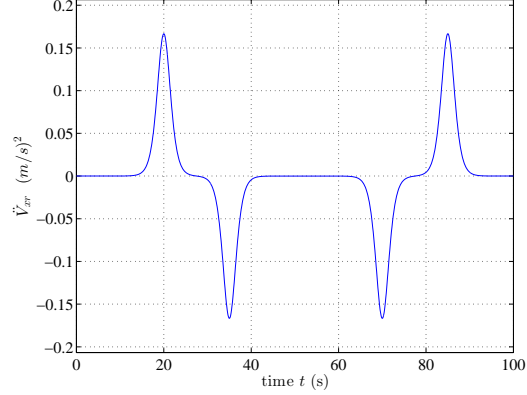
FIG. 11: The second derivative $\ddot{V}_{xr} = \ddot{\Omega}_{\boldsymbol{p}_u, \boldsymbol{p}_d}$ (jerk).

We then set

$$\Delta_{Vu} = V_{hu} - V_{lu}, \quad \Delta_{Vd} = V_{hd} - V_{ld}, \qquad \Delta_{tu} = t_{eu} - t_{bu}, \quad \Delta_{td} = t_{ed} - t_{bd}$$

$$\dot{V}_{xm} = -\frac{\Delta_{Vd}}{\Delta_{td}}, \quad \dot{V}_{xM} = \frac{\Delta_{Vu}}{\Delta_{tu}}, \quad \ddot{V}_{xm} = -\max\left(\frac{\sigma_u \Delta_{Vu}}{\Delta_{tu}}, \frac{\sigma_d \Delta_{Vd}}{\Delta_{td}}\right), \quad \ddot{V}_{xM} = -V_{xm}$$

5.2 *Torque expression and simple bounds*

We shall give in this Subsection various bounds, postponing a discussion about them to Subsection 5.3, p. 12.

5.2.1 *Torque expression amenable to be bounded.*   Recall the expression obtained for the trajectory tracking feedback law in Eq. (4.1):

$$T = \frac{1}{R}\left[\left(mr + \frac{I_w \omega}{V_x}\right)\dot{V}_x + F_o - \frac{I_w \max\left(r^2 \omega^2, V_x^2\right)}{grV_x \mu_x'}\ddot{V}_x\right]$$

Then, we have:

- In the acceleration case, where $r\omega \geqslant V_x$, $\lambda \leqslant 0$

$$\frac{\omega}{V_x} = \frac{1}{r(1+\lambda)}$$

- In the deceleration case, where $r\omega \leqslant V_x$, $\lambda \geqslant 0$

$$\frac{\omega}{V_x} = \frac{1-\lambda}{r}$$

Thus, the expression for the torque is

- In the acceleration case

$$T = \frac{1}{R} \left[\left(mr + \frac{I_w}{r(1+\lambda)} \right) \dot{V}_x + F_o + \frac{I_w}{gr\mu'_x(1+\lambda)^2} V_x \ddot{V}_x \right]$$

- In the deceleration case

$$T = \frac{1}{R} \left[\left(mr + \frac{I_w(1-\lambda)}{r} \right) \dot{V}_x + F_o - \frac{I_w}{gr\mu'_x} V_x \ddot{V}_x \right]$$

5.2.2 *Generic bound.* We have the following bounds for $|T|$:

- In the acceleration case

$$|T| \leqslant \frac{1}{R} \left[\left(mr + \frac{I_w}{r(1+\lambda)} \right) \dot{V}_x + |F_o| + \frac{I_w}{gr|\mu'_x|(1+\lambda)^2} V_x |\ddot{V}_x| \right] \tag{5.6}$$

- In the deceleration case

$$|T| \leqslant \frac{1}{R} \left[\left(mr + \frac{I_w(1-\lambda)}{r} \right) |\dot{V}_x| + |F_o| + \frac{I_w}{gr\mu'_x} V_x |\ddot{V}_x| \right] \tag{5.7}$$

5.2.3 *A simplistic bound.* A simplistic bound is given by considering minimum (in denominators) and maximum (in numerators) values for the various expressions in the bounding formulas (5.6)–(5.7):

- In the acceleration case

$$|T| \leqslant \frac{1}{R} \left[\left(mr + \frac{I_w}{r(1+\lambda_m)} \right) \dot{V}_{xM} + \frac{I_w}{gr|\mu'_{xm}|(1+\lambda_m)^2} V_{xM} |\ddot{V}_{xM}| \right] \tag{5.8}$$

- In the deceleration case

$$|T| \leqslant \frac{1}{R} \left[\left(mr + \frac{I_w(1-\lambda_m)}{r} \right) |\dot{V}_{xM}| + \frac{I_w}{gr\mu'_{xm}} V_{xM} |\ddot{V}_{xM}| \right] \tag{5.9}$$

with the following notations (see, in particular, Eq. (4.9))

$$\dot{V}_{xM} = \max \left(\frac{\Delta_{Vu}}{\Delta_{tu}}, \frac{\Delta_{Vd}}{\Delta_{td}} \right), \qquad \ddot{V}_{xM} = \max \left(\frac{\sigma_u \Delta_{Vu}}{\Delta_{tu}}, \frac{\sigma_d \Delta_{Vd}}{\Delta_{td}} \right) \tag{5.10}$$

$$\lambda_m = -\lambda_M = \mu^{-1}(\mu_M) = -\lambda^* + \varepsilon_\lambda, \quad \mu'_m = \mu'(\lambda^* - \varepsilon_{\mu'}) \tag{5.11}$$

5.2.4 *A simple but realistic bound.* We shall then consider the following more realistic bounding function:

- In the acceleration case

$$|T| \leqslant \left(\frac{mr}{R} + \frac{I_w}{rR(1+\lambda_m)} \right) \dot{V}_x + \max \left(\frac{I_w V_{xr} |\ddot{V}_{xr}|}{grR|\mu'_{xr}|(1+\lambda_r)^2} \right) = \xi_{aM} \dot{V}_x + \zeta_{aM} \tag{5.12}$$

- In the deceleration case

$$|T| \leqslant \left(\frac{mr}{R} + \frac{I_w(1-\lambda_m)}{rR} \right) |\dot{V}_x| + \max \left(\frac{I_w V_{xr} |\ddot{V}_{xr}|}{grR\mu'_{xr}} \right) = \xi_{dM} \dot{V}_x + \zeta_{dM} \tag{5.13}$$

5.3 *Discussion and bounds fulfilment*

5.3.1 *Generic bound.* The bound given in Equations (5.6)–(5.7) is rather generic, since it contains expressions in λ, yielding expressions in V_x (see, e.g. Eq. (3.2)). Thus, it cannot be used very simply.

5.3.2 *Simplistic bound.* The simplistic bound of Equations (5.8)–(5.9) are far too pessimistic. Indeed, e.g. for the trajectory given in Figure 4, p. 8, the above bound in the acceleration case is 9696.828N, when the real maximum on T is 1.948N. It is thus unusable.

5.3.3 *A simple but realistic bound.* The simple bound given in Equations (5.12)–(5.13) yields a maximum of 1.962N which is a much better bound than the previous one, wrt the real maximum of 1.948N.

REMARK 5.1 Note that the bounding functions (5.12)-(5.13) are valid for any type of reference trajectory, and not only the one given in (4.5), p. 6.

Recall the form of the bounds given in (5.3)

$$\dot{V}_{xm} = -\frac{\Delta_{Vd}}{\Delta_{td}}, \quad \dot{V}_{xM} = \frac{\Delta_{Vu}}{\Delta_{tu}}$$

$$\Delta_{Vu} = V_{hu} - V_{lu}, \quad \Delta_{Vd} = V_{hd} - V_{ld}, \quad \Delta_{tu} = t_{eu} - t_{bu}, \quad \Delta_{td} = t_{ed} - t_{bd}$$

and suppose Δ_{Vu} and Δ_{Vd} being given by practical considerations (e.g. speed limits). From the bounds obtained in (5.12)–(5.13), we then have

- In the acceleration case

$$|T| \leqslant \xi_{aM}\dot{V}_x + \zeta_{aM} \leqslant \xi_{aM}\dot{V}_{xM} + \zeta_{aM} = \xi_{aM}\frac{\Delta_{Vu}}{\Delta_{tu}} + \zeta_{aM} \tag{5.14}$$

- In the deceleration case

$$|T| \leqslant \xi_{dM}\dot{V}_x + \zeta_{dM} \leqslant -\xi_{dM}\dot{V}_{xm} + \zeta_{dM} = \xi_{dM}\frac{\Delta_{Vd}}{\Delta_{td}} + \zeta_{dM} \tag{5.15}$$

Then, to ensure some prescribed bound on the the torque

$$|T| \leqslant T_{Ma} \text{ on acceleration, and } |T| \leqslant T_{Md} \text{ on deceleration} \tag{5.16}$$

it is sufficient to impose the following bounds on Δ_{tu}, Δ_{td}:

$$\Delta_{tu} > \frac{\xi_{dM}\Delta_{Vd}}{T_{Md} - \zeta_{dM}}, \qquad \Delta_{ta} > \frac{\xi_{aM}\Delta_{Va}}{T_{Ma} - \zeta_{aM}}$$

In Figure 12, we have the bounds (5.12)–(5.13) in dashed line ($\xi_{aM}\dot{V}_x + \zeta_{aM}$ and $\xi_{dM}\dot{V}_x + \zeta_{dM}$) and the torque T in solid line, and in Figure 13 is depicted the error between the previous two. Note that the maximum error is $1.398.10^{-2}$, which is 0.18% of T_r's maximum.
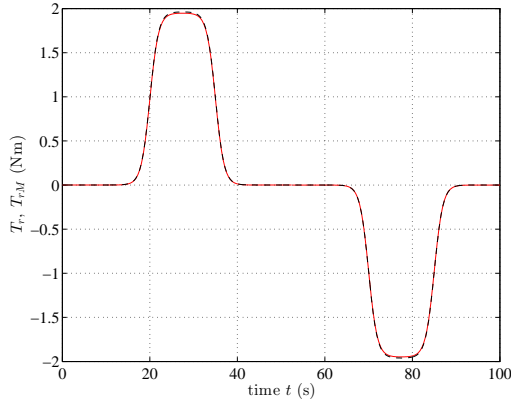
FIG. 12: Bounds (5.12)–(5.13) on T.
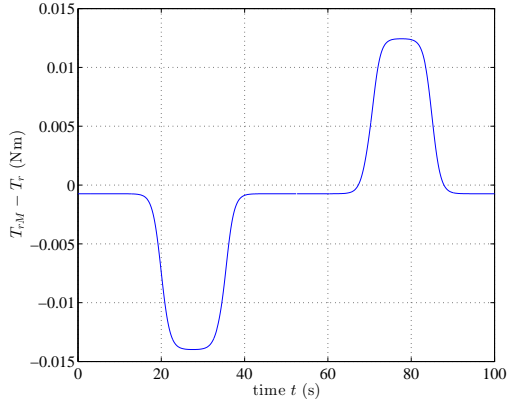
FIG. 13: Error between T and the bounds (5.12)–(5.13).

6. Conclusion

We have elaborated a simple yet efficient scheme for tracking a reference speed of a longitudinal vehicle model with torque constraint. The flatness character of the model enabled to embed the constraint fulfilment in the trajectory design. We considered a special class of functions for the class output, namely combinations of $\log(\cosh(t))$ type functions.

More general classes of functions will be considered in the future, together with some other types of constraints.

References

Egbert Bakker, Lars Nyborg, and Hans B. Pacejka. Tyre modelling for use in vehicle dynamics studies. In *SAE Technical Paper*. SAE International, 02 1987.

Maria Bekcheva, Luca Greco, Hugues Mounier, and Alban Quadrat. Euler-bernoulli beam flatness based control with constraints. In *Proc. of IEEE 9th International Workshop on Multidimensional (nD) Systems (IEEE nDS 2015)*, Vila Real, Portugal, 2015.

Maria Bekcheva, Hugues Mounier, and Luca Greco. Control of differentially flat linear delay systems with constraints. In *Proc. of 20th IFAC World Congress*, Toulouse, France, 2017.

Abbas Chamseddine, Ddidier Theilliol, Youmin Zhang, Cédric Join, and Camille-Alain Rabbath. Active fault-tolerant control system design with trajectory re-planning against actuator faults and saturation: Application to a quadrotor unmanned aerial vehicle. *International Journal of Adaptive Control and Signal Processing*, 29(1):1–23, 2013. doi: 10.1002/acs.2451.

J.R. Ellis. *Vehicle dynamics*. Business Books, 1969.

Nadeem Faiz, Sunil K. Agrawal, and Richard M. Murray. Trajectory planning of differentially flat systems with dynamics and inequalities. *Journal of Guidance, Control, and Dynamics*, 24(2):219–227, 2001. doi: 10.2514/2.4732.

Michel Fliess, Jean Levine, Philippe Martin, and Pierre Rouchon. Flatness and defect of nonlinear systems: introductory theory and examples. *Internat. J. Control*, 61:1327–1361, 1995.

Melvin E. Flores and Mark B. Milam. Trajectory generation for differentially flat systems via NURBS basis functions with obstacle avoidance. In *2006 American Control Conference*, 2006. doi: 10.1109/acc.2006.1657645.

T.D. Gillespie. *Fundamentals of Vehicle Dynamics*. Premiere Series Bks. Society of Automotive Engineers, 1992.

Ling-Yuan Hsu and Tsung-Lin Chen. An optimal wheel torque distribution controller for automated vehicle trajectory following. *IEEE Transactions on Vehicular Technology*, 62(6):2430–2440, 2013. doi: 10.1109/tvt.2013.2246593.

Ling-Yuan Hsu, K Weng, and Tsung-Lin Chen. A constrained wheel torque controller for lane following system using control distribution. In *Proceedings of the 2010 American Control Conference*, 2010. doi: 10.1109/acc.2010.5530720.

Nazli E. Kahveci and Petros A. Ioannou. Cruise control with adaptation and wheel torque constraints for improved fuel economy. In *2010 IEEE Intelligent Vehicles Symposium*, 2010. doi: 10.1109/ivs.2010.5547986.

Alexander Keck, Karl Lukas Knierim, and Oliver Sawodny. SAMMY - an algorithm for efficient computation of a smooth path for reference trajectory generation. In *2015 6th International Conference on Automation, Robotics and Applications (ICARA)*, 2015. doi: 10.1109/icara.2015.7081133.

Uwe Kiencke and Lars Nielsen. *Automotive Control Systems: For Engine, Driveline and Vehicle*. Springer-Verlag New York, Inc., Secaucus, NJ, USA, 1st edition, 2000.

Shengbo Li, Keqiang Li, Rajesh Rajamani, and Jianqiang Wang. Model predictive multi-objective vehicular adaptive cruise control. *IEEE Transactions on Control Systems Technology*, 19(3):556–566, 2011. doi: 10.1109/tcst.2010.2049203.

Johannes Löwis and Joachim Rudolph. Real-time trajectory generation for flat systems with constraints. In *Nonlinear and Adaptive Control*, volume 281, pages 385–394. Springer, Berlin, Heidelberg, 2003. doi: 10.1007/3-540-45802-6_31.

Lghani Menhour, Brigitte d'Andréa Novel, Michel Fliess, and Hugues Mounier. Coupled nonlinear vehicle control: Flatness-based setting with algebraic estimation techniques. *Control Engineering Practice*, 22:135–146, 2014. doi: 10.1016/j.conengprac.2013.09.013.

Henning Mitschke, Manfred ; Wallentowitz. *Dynamik der Kraftfahrzeuge*. Springer, 2004.

H.B. Pacejka. *Tyre and Vehicle Dynamics*. Automotive engineering. Butterworth-Heinemann, 2006.

Nicolas Petit and Antonio Sciarretta. Optimal drive of electric vehicles using an inversion-based trajectory generation approach. *IFAC Proceedings Volumes*, 44(1):14519–14526, 2011. doi: 10.3182/20110828-6-it-1002.01986.

R. Rajamani. *Vehicle Dynamics and Control*. Mechanical Engineering Series. Springer US, 2011.

Michael Ross and Fariba Fahroo. Pseudospectral methods for optimal motion planning of differentially flat systems. *IEEE Transactions on Automatic Control*, 49(8):1410–1413, 2004. doi: 10.1109/tac.2004.832972.

Thomas Ruppel, Karl Lukas Knierim, and Oliver Sawodny. Analytical multi-point trajectory generation for differentially flat systems with output constraints. *IFAC Proceedings Volumes*, 44(1):950–955, 2011. doi: 10.3182/20110828-6-it-1002.00527.

Sophie Tarbouriech and Matthew Turner. Anti-windup design: an overview of some recent advances and open problems. *IET Control Theory & Applications*, 3(1):1–19, 2009. doi: 10.1049/iet-cta:20070435.

Stephanie Tsuei and Mark B. Milam. Trajectory generation for constrained differentially flat systems with time and frequency domain objectives. In *2016 IEEE 55th Conference on Decision and Control (CDC)*, 2016. doi: 10.1109/cdc.2016.7798902.

Giorgio Valmorbida, Sophie Tarbouriech, and Germain Garcia. Design of polynomial control laws for polynomial systems subject to actuator saturation. *IEEE Transactions on Automatic Control*, 58(7): 1758–1770, 2013. doi: 10.1109/tac.2013.2248256.

Jorge Villagra, Brigitte d'Andréa Novel, Michel Fliess, and Hugues Mounier. Estimation of longitudinal and lateral vehicle velocities: An algebraic approach. In *2008 American Control Conference*, pages 3941–3946, Seattle, Washington, USA, 2008. IEEE. doi: 10.1109/acc.2008.4587108.

Rahee Walambe, Nipun Agarwal, Swagatu Kale, and Vrunda Joshi. Optimal trajectory generation for car-type mobile robot using spline interpolation. *IFAC-PapersOnLine*, 49(1):601–606, 2016. doi: 10.1016/j.ifacol.2016.03.121.